Yeast D–Amino Acid Oxidase: Structural Basis of its Catalytic Properties

Mirella S. Pilone, Gianluca Molla, Loredano Pollegioni
Dept. Structural Functional Biology, University Insubria, via Dunant 3, Varese, Italy
Kay Diederichs, Wolfram Welte, Sandro Ghisla
Section of Biology, University Konstanz, P.O. Box 5560–M644, Konstanz, Germany

Introduction

D–amino acid oxidase (DAAO) has played a prominent role in the development of present concepts in mechanistic enzymology and biochemistry. The enzyme catalyses the deamination of D–amino acids to their imino acid counterparts with concomitant reduction of FAD. The reduced flavin is subsequently reoxidized by O_2 generating H_2O_2. The imino acid is released into solvent where it spontaneously hydrolyses to the corresponding α–keto acid and ammonia.

Yeast and mammalian DAAO's have been widely characterized and they share features such as the same basic catalytic mechanism. However, they differ in important aspects such as catalytic efficiency, substrate specificity, aggregation state, stability, kinetic mechanism, and mode and effectiveness of FAD binding (1). While yeast DAAO exists in a stable dimeric state, pkDAAO dissociates easily and releases the FAD cofactor concomitant with loss of activity. DAAO from the yeast *Rhodotorula gracilis* (RgDAAO) has a k_{cat} of 20,000 min^{-1} compared to 600 min^{-1} for pig kidney DAAO (pkDAAO) with D–alanine as substrate. This diversity arises mainly from a different rate–limiting step in the catalytic cycle. It is flavin reduction with RgDAAO and product release with pkDAAO.

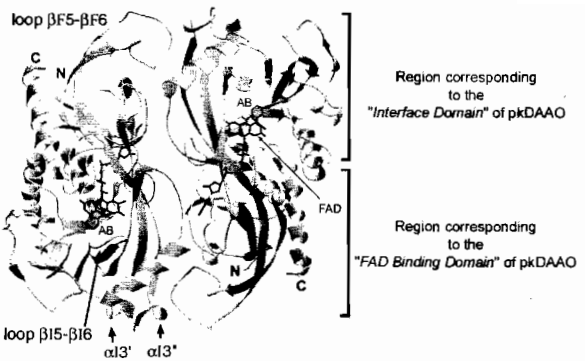

Figure 1: Ribbon representation of RgDAAO–anthranilate complex (PDB accession code 1c0i) with the proposed 'head to tail' dimer. The additional structural elements not present in pkDAAO are indicated.

The understanding of the molecular basis for these similarities and differences was the rationale for the present work. In this context we consider the crystal structure of RgDAAO in complex with the competitive inhibitor anthranilate (*o*–aminobenzoate) in relation to the other crystal structures of the enzyme in complex with D–alanine and CF_3–D–alanine and to the catalytic properties of RgDAAO. A full account of these data has been submitted (L. Pollegioni et al., 2002). The structures of pkDAAO (2) and LAAO (3) in complex with anthranilate have also been solved; comparison of the modes of interaction of this ligand with the three enzymes provides further insights into similarities and differences of structure–function relationships of these flavoenzymes.

Materials and methods

Recombinant RgDAAO was expressed and purified in *E. coli* using the pT7–DAAO expression system in BL21(DE3)pLysS *E. coli* cells. The purified protein was concentrated up to 10 mg/ml and equilibrated in 20 mM HEPES buffer at pH 7.5. The dynamic light scattering analysis was performed with model DynaPro 801 (Protein Solutions Ltd.). The recombinant form of RgDAAO was crystallized by vapor diffusion method at 18 °C, as reported in (4). The RgDAAO–anthranilate complex was obtained by soaking the crystals in the cryo–protection solution containing 30 mM of the ligand. Data collection, under cryogenic conditions, was performed on a rotating anode source (Schneider, Offenburg, Germany) using the MAR345 image plate system. Space group determination and data reduction was carried out in XDS. The refined model of the RgDAAO–lactate complex (1c0k) was the starting point for solving the structure of RgDAAO in anthranilate complex. The refinement employed a torsion angle dynamics at a starting temperature of 5,000 K. Refinement was continued with SHELXL. The restraints were set in accordance with the resolution of the data and continuous control of the stereochemical quality of the structures was done with PROCHECK.

Results and discussion

Overall structure and topology

The RgDAAO used for the present studies is a chimeric protein containing six additional residues (MARIRL) at the N–terminus in addition to the 368 amino acids of the native form (1). The 3D–structure of the complex obtained in the presence of anthranilate is depicted in Fig. 1. While there is correspondence between the FAD binding domain for the Rg– and pkDAAOs, differences at the interface domain (denoted with "I") lead to a different mode of dimer formation (see below). The secondary structure topology consists of 11 α–helices and 13 β–strands; it is overall analogous to that of pkDAAO (2). Two domains are present and their main structural element is a central antiparallel β–sheet. Compared to pkDAAO, in RgDAAO there are three additional short α–helices: according to (2), these can be named αI1' (between βI1 and βI2), αI3' and αI3'' (both after αI3). Two main topological

differences are also evident: the presence of a significantly shorter active site loop connecting βI5 and βI6 (6 residues in RgDAAO *vs.* 11 residues in pkDAAO) (Fig. 2A and C), and the presence of a long C–terminal loop (21 amino acids connecting βF5 and βF6). The latter is not present in other known DAAO sequences.
Based on structural and sequence homologies, RgDAAO can be classified as a member of the large glutathione reductase (GR family) into the subgroup GR_2 (5). In the case of the comparisons of RgDAAO and pkDAAO, the r.m.s deviation of 1.38 Å for 281 superimposable C–alpha atoms (within a 3.5 Å cut–off) is surprisingly high and reflects the evolutionary distance between the mammalian and the yeast enzyme (see Table 1). No correlation between the r.m.s. deviation and the percentage of superimposed residues is evident from comparing RgDAAO with other GR_2 family members. This might hint at the large mutual evolutionary distance of members within this family.
At the N–terminus only two (RL) out of six of the additional amino acids (MARIRL) can be modelled into the electron density map, the remaining four apparently possessing a flexible conformation. This segment appears to be a significant component in crystal formation and growth since we have failed to obtain crystals of wild–type protein. In the long loop connecting βF5 and βF6 (Fig. 1) the electron density for eight amino acids (Arg312–Gln319) is also weak, indicating that part of the loop is very flexible. Even the C–terminal residues Ala362–Leu368 are not visible in the electron density; this region contains the SKL tripeptide, the PTS1 targeting sequence for peroxisomal proteins.
In RgDAAO the FAD is found in an extended conformation typical of this GR family, and the binding domain contains the conserved βαβ motif (Rossman fold). The whole cofactor is buried inside the protein (Fig. 1) and is not solvent accessible in agreement with previous data on the absence of reactivity of the enzyme reconstituted with modified FAD analogues (1). The isoalloxazine ring is located at the interface of the two domains, with the *re*–side facing the inner part of the substrate–binding cavity. The flavin N(1) is also within H–bond distance with Ser335(=O), such an interaction being absent in pkDAAO, and four H_2O molecules are found at optimal distance for

Table 1: Comparison of RgDAAO with other Members of the GR_2 Family.

	pkDAAO	SOx	PH	pHBH	LAAO	CO
Residues within 3.5 Å cutoff (number)	281	193	121	120	120	110
r.m.s deviation of residues within 3.5 Å cutoff	1.38	1.66	1.75	1.65	1.70	1.87
Sequence identity of residues within 3.5 Å cutoff (%)	31.8	18.7	17.4	19.2	24.4	20.4

pkDAAO: mammalian D–Amino acid oxidase (1aa8); SOx: Sarcosine oxidase (1b3m_a); PH: Phenol hydroxylase (1foh); pHBH: p–Hydroxybenzoate hydroxylase (1bf3); LAAO: L–Amino acid oxidase (1f8r); CO: Cholesterol oxidase (1b4v).

H–bond formation with three of the phosphate oxygen atoms. Thus, although different amino acids interact with AMP in yeast and mammalian enzyme, the overall picture is similar in the two DAAO's.

Mode of dimerization

Native DAAO from *R. gracilis* is a stable 80 kDa dimer of identical subunits, independent from the protein concentration (1). In contrast to this, the apoprotein form of RgDAAO is monomeric and rapidly converts to dimeric holoenzyme upon addition of FAD: it can be deduced that dimerization follows holoenzyme reconstitution. The similarity between the molecular weight estimated by dynamic light scattering (≈79 kDa) and the theoretical value of 82 kDa for the recombinant enzyme is consistent with RgDAAO as a roughly spherical homodimer in solution. The mode of dimerization cannot be derived directly from space group crystal symmetry. In the 3D–structure, the monomer of the asymmetric unit makes crystal contacts to give three symmetry–related dimers indicating different, possible modes of monomer–monomer interaction. The largest buried surface (3,049 $Å^2$) (calculated using the CNS software package) is obtained for a "head to tail" monomer orientation with C2 symmetry (Fig. 1) that is different from that reported for mammalian DAAO (2). Notably, loop βF5–βF6 of yeast DAAO, not conserved in other DAAO sequences, appears to play an important role in monomer–monomer interaction. It is largely due to electrostatic interactions of positively charged residues of this long loop with negatively charged ones belonging to two additional α–elices, also not conserved, αI3' and αI3" of a symmetry related monomer. This different mode of oligomerisation probably causes the differences in stability and tightness of FAD cofactor binding between the DAAO's from different sources.

The active site cavity

The active site of RgDAAO is a cavity delimited by the two long β–strands I4 and I8 (see Fig. 2A) where the flavin forms the "bottom" of the cavity. The side chains of Phe58, Ser215, Pro221, and the backbone of Ser234 and Ser235 form the entrance to the active site whose opening is controlled by the orientation of the phenolic ring of Tyr238 (see below), and also provides a surface suitable to interact with non–polar and aromatic compounds (and substrates). The anchoring of the ligand carboxylate with Arg285 and Tyr223 is found for all RgDAAO complexes studies (Fig. 2A) (4). The comparison of the active center of yeast and mammalian DAAO in complex with anthranilate is shown in Fig. 2B and C. Interestingly the loop found in pkDAAO, which was proposed to act as a "lid" controlling access to the active site (Fig. 2C) (2) is absent in RgDAAO. In the RgDAAO–CF_3–D–alanine complex, the Tyr238 side chain is placed at a similar position of Tyr224 of pkDAAO (compare Fig. 2A and C) even if located on a different segment of the main chain.

In the RgDAAO–anthranilate complex, two molecules of anthranilate are found at the active site. One is placed in the vicinity of the flavin N(5), and the second is located at the entrance of the active site cavity. Comparison of the binding mode of the first anthranilate with that of CF_3–D–alanine (4) shows that two significant differences are evident: in the RgDAAO–anthranilate complex, Tyr238 has moved away from the ligand $–COO^-$ and it is too distant to make any discrete H–contact(s) with the latter;

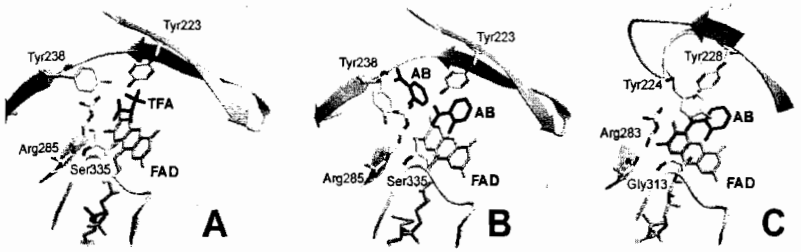

Figure 2: The active site of RgDAAO in complex with CF_3–D–alanine (A) and anthranilate (B); the active site of pkDAAO in complex with anthranilate (C).

displacement of active site Wat72 in the DAAO–anthranilate complex occurs due to the bulkiness of the ligand. The second anthranilate molecule lies parallel to, and in contact with, the phenolic ring of Tyr238. Therefore, while Tyr238–OH interacts with the carboxylate of the quasi–substrate CF_3–D–alanine (4) (Fig. 2A), in the anthranilate complex it rotates opening the entrance of the active site, and interacts there with the second bound anthranilate (Fig. 2B). This serves in channelling substrate to the active site bottom, the locus of chemical catalysis. The "lid" covering the active site in pkDAAO has been proposed to regulate product dissociation, while the side chain of Tyr238 might exert a similar role in RgDAAO, where the lid is absent, yielding to the differences in kinetic mechanism observed between the two enzymes. In analogy to LAAO, where three anthranilate molecules are present in each protomer inside the channel leading to the active site (3), the position of the two anthranilate molecules found in RgDAAO could reflect the trajectory of the substrate from the surface to the locus of the catalytic event (Fig. 2B). With RgDAAO, no arrangement of (partial) positive charges that could stabilise the flavin N(1) is evident from the 3D–structure. To account for stabilization we proposed that Arg285 plays a dual role (6). In the presence of a ligand having a carboxylic group it serves in its binding. In the free enzyme form, the guanidinium side chain of Arg285 rotates around the Cε bond to come in close proximity (≈3 Å) to the flavin ring and above its plane, where it can exert a neutralizing function. Modelling studies show that with pkDAAO the equivalent Arg283 can do the same (not shown).We would thus infer that also with pkDAAO the stabilisation of negatively charged flavin pyrimidine species results primarily from the interaction with this Arg, whereby the invoked helix dipole (2) can play an ancillary role.

In conclusion, comparison of the 3D–structures of yeast and mammalian DAAO suggests that evolutive pressure has led to two enzymes that share the same chemical process, but use different kinetic mechanisms for catalysis. In the case of RgDAAO, and as a consequence of catabolic requirements (1), optimal catalytic efficiency has evolved leading to the (chemical) step of hydride transfer being rate limiting. With

mammalian DAAO we assume that the necessity to modulate activity has caused the product release step to be limiting. This diversity is mainly implemented by the use of different types of "lids" that cover the active site and are involved in uptake and release of the ligand/substrate.

Acknowledgements. This work was supported by a grant from Italian MIUR to Dr. M.S. Pilone (PRIN 2000–2002 Prot. MM05C73482). The CPU consuming calculations with a parallel version of SHELXL were performed on a SGI Origin 2000 at the University of Freiburg, Germany.

References

1. Pilone M.S. (2000): D–amino acid oxidase: new findings. Cell. Mol. Life Sci. **57**, 1732–1747.

2. Mattevi A., Vanoni M.A., Todone F., et al. (1996): Crystal structure of D–amino acid oxidase: a case of active site mirror–image convergent evolution with flavocytochrome b_2. Proc. Natl. Acad. Sci. USA **93**, 7496–7501.

3. Pawelek P.D., Cheah J., Coulombe R., et al. (2000): The structure of L–amino acid oxidase reveals the substrate trajectory into an enantiomerically conserved active site. The EMBO J. **19**, 4204–4215.

4. Umhau S., Pollegioni L., Molla G., et al. (2000): The X–ray structure of D–amino acid oxidase at very high resolution identifies the chemical mechanism of flavin–dependent substrate dehydrogenation. Proc.Natl. Acad. Sci. USA **97**, 12463–12468.

5. Dyn O., Eisenberg D. (2001): Sequence–structure analysis of FAD–containing proteins. Protein Sci. **10**, 1712–1728.

6. Molla G., Porrini D., Job V., et al. (2000): Role of arginine 285 in the active site of *Rhodotorula gracilis* D–amino acid oxidase. A site–directed mutagenesis study. J. Biol. Chem. **275**, 24715–24721.